Contents lists available at Egyptian Knowledge Bank
Microbial Biosystems
Journal homepage: http://mb.journals.ekb.eg/

Protein structure and its effects on transcription in *Zymobacter palmae* and *Escherichia coli* for ethanol production

Kathiresan Subramanian[1*], Kagne Suresh[2]

[1*]*Hospira Healthcare Pvt. Ltd, Chennai, Tamil Nadu 600017, India.*
[2]*Badrinarayan Barwale Mahavidhyalaya, Jalna, Maharashtra 431213, India.*

ABSTRACT

Zymobacter palmae, a Gram-negative bacterium from the *Halomonadaceae* family, is a facultative anaerobic and mesophilic organism. It is extremely rare and has been researched for its unusual capacity to contribute to natural fermentation processes, resulting in different compounds. *Z. palmae* can efficiently make ethanol by breaking down simple sugars and carbohydrates, such as monosaccharides and oligosaccharides. It also contains enzymes such as cellulase, protease, and lyase, all of which are essential for ethanol formation. The study also examined the stability of these enzymes in a wild *E. coli* strain and compared the results with *Z. palmae*. However, structural information on these enzymes remains unavailable. The principal objective of the learning focused onto model and validate three-dimensional (3D) structures of cellulase, protease, and lyase enzymes in *Z. palmae*, with a focus on understanding their structural characteristics and functional significance in ethanol production. The National Center for Biotechnology Information (NCBI) database provided the annotated genomic sequence of *Z. palmae* and *E. coli* for this study. The CGview program revealed the organism's circular genome structure. Protein modeling and secondary structure analysis were done with AlphaFold2 and NetSurfP, respectively. A molecular dynamic simulation (MDS) study was also evaluated using the WebGRO program. The outcomes exhibited excellent confidence on projected local distance difference test (pLDDT) scores: 95.2% for cellulase, 91.9% for lyase, and 93.2% for protease. MDS analysis at 50 nanoseconds (ns) validated the structural stability of cellulase, lyase, and protease, with RMSD values of around 0.2 nm, 0.8 nm, and 0.5 nm respectively. These findings imply that *Z. palmae* can manufacture stable enzymes, hence contributing to long-term ethanol synthesis. Some of the *Z. palmae* ethanol production key enzymes were comparable with the wild strain of *E. coli*.

Introduction

Fossil fuels have been the primary source of energy for the past two centuries. Their finite resources and increasing use every year create future challenges with fuel energy-related concerns (Wang & Azam 2024). By the end of the twenty-first century, fossil fuel resources are expected to be depleted (Holechek et al. 2022). As a result, improving biofuel production through sustainable ways is critical (Liu et al., 2021). In this context, microbial-driven enzymatic conversion appears to be a promising alternate technique for addressing the problem (Zheng et al., 2024). Number of research studies have revealed that trial run demonstrated manufacture of

ethanol (EtOH) from biomass and boost microorganisms such as *Escherichia coli* (Abdel-Salam et al., 2023), *Erwinia chrysanthemi* (Piriya et al., 2012) & *Klebsiella oxytoca* (Tao et al., 2019). These microbes carry the pet operon on their plasmids or chromosomes, which is essential for EtOH synthesis from cellulosic sources. Despite substantial study, producing higher EtOH yields on a commercial scale remains a difficulty. Exploring novel genes through whole genome research of other microorganism offers a prospect to evaluate enzyme stability and efficiency. Identifying and incorporating these genes into modified bacterial strains may greatly improve EtOH production, opening the path for more sustainable and commercially viable biofuel alternatives. The wild strain of *Z. palmae* was initially isolated from palm sap (Okamoto et al., 1993). This microbe has sparked widespread scientific attention due to its amazing metabolic capabilities and various enzymatic pathways, which include homofermentative metabolism (Quinn et al., 2019). Its metabolic pathways, which are controlled by individual genes, are well-known for their involvement in fermentation and EtOH synthesis. This critical function not only improves biofuel production but also has potential for a variety of biotechnological applications (Panahi et al., 2022).

Fermentation processes are classified according to the physical state of the biomass. The first stage comprises suspended liquid-phase fermentation, which is extensively employed in industrial applications with stirred reactors. Planktonic microbial cells grow freely, producing both biomass and metabolites (Todhanakasem et al., 2019). The following stage is sessile-state fermentation, in which bacteria form biofilms—structured colonies immersed in a polysaccharide matrix and adhering to surfaces. Biofilms have long been used for wastewater treatment, bioremediation, and off-gas purification (Philipp et al., 2023). Furthermore, biofilms show significant promise for the long-term manufacturing of bio-based products. Their advantages include fast fermentation rates, structural compactness, efficient recycling, high resistance to hazardous inhibitors, and sustained enzymatic activity, all of which help to reduce manufacturing costs (Leonov et al., 2021). Biofilms have recently gained recognition as effective biocatalysts in industrial manufacturing, allowing for the production of biofuels, chemicals, amino acids, antibiotics, surfactants, exopolysaccharides, and other valuable secondary metabolites (Todhanakasem et al., 2019; Philipp et al., 2023).

Z. palmae and *E. coli* may ferment a variety of substrates, including hexose, c-linked di- and tri-saccharides, and sugar alcohols (Kojima et al., 2013). Notably, maltose fermentation is extremely efficient,

with 15% of maltose being transformed. Glucose concentrations above 10% cause delayed fermentation onset and reduced culture development (Bušić et al., 2018). *Z. palmae* has a unique metabolic pathway centered on the enzyme pyruvate decarboxylase (PDC), which converts pyruvate into CO_2 and acetaldehyde. This emphasizes its evolutionary distinctiveness and metabolic plasticity (Quinn et al. 2019). The obtained crystal structure of PDC (PDB ID: 5EUJ) providing vital insights into its function and establishing the framework for future research of metabolic complexity (Alcover et al., 2019). Aside from PDC, *Z. palmae* has a broad variety of enzymes, including cellulase, protease, and lyase, which are required for EtOH synthesis.

However, the lack of specific structural information on these enzymes has restricted our knowledge of their metabolic operations. Gaining thorough insights into their structural and functional roles will greatly increase our understanding of EtOH production, potentially leading to better biofuel-generating strategies. *Z. mobilis* AX101, *E. coli* KO11, and *S. cerevisiae* 424A (LNH-ST) are already reported organisms that are capable of producing ethanol between 82.4% and 93.2% of metabolic theoretical yield metabolic yield (Lau et al., 2010).

The scope of this research is to model and validate the 3D structures of cellulase, protease, and lyase enzymes in *Z. palmae* and *E. coli* using NCBI genomic data and advanced structural bioinformatics tools. It also aims to clarify structural and functional functions of these enzymes in EtOH generation, providing insights into optimizing biotechnological uses and promoting sustainable biofuel production. The findings of this study will enhance our understanding of the metabolic structure of *Z. palmae* and lay the groundwork for future experimental advancements in ethanol production upon comparison with *E. coli* for the eligibility of an ideal organism for potential candidate organism for large scale ethanol production.

Materials and Methods
Retrieval of genome sequence
The genome sequence of *Zymobacter palmae* was retrieved from the NCBI database (https://www.ncbi.nlm.nih.gov/datasets/genome/GCF_003610015.1/) and , with the NCBI RefSeq assembly number GCF_003610015.1 and *E. coli* from wild strain was retrieved from PRJNA1138183.. Utilizing the annotated genome file, a circular representation displaying coding regions, non-coding regions, tRNA, GC content, and total base pairs was generated using the CGview webserver (Grant & Stothard, 2008).

Protein modeling

The ChimeraX version 1.4 software package (Pettersen et al., 2021) was used to predict three-dimensional (3D) protein structures based on amino acid sequences using the AlphaFold2 tool. The structure determination process included selecting AlphaFold2 from the software's tools area. In essence supplying input of amino acid sequence onto query box is required for running the prediction with the default parameters. The resulting tertiary protein structures were then assessed for stereochemical quality with the PROCHECK tool (Laskowski et al., 1993), which produced a Ramachandran plot for validation.

Secondary Structure Prediction

The NetSurfP tool visualized secondary protein structure by supplying amino acid sequences in FASTA format with default parameters, as described by Høie et al. (2022).

Evaluation of physical and chemical properties of enzymes

The amino acid sequences were converted to FASTA and entered into the query box of ExPASy's ProtParam server (Gasteiger, 2003). Following submission, the server examined the sequences to identify different physiochemical parameters, including number of negatively charged residues, molecular weight, instability index, isoelectric point (pI), total amino acid composition, and average hydropathicity.

Active site prediction

Before docking, identifying the specific active site of each protein is crucial, as the ligand binds to this region. The PrankWeb server (https://prankweb.cz/) was employed to envisage the dynamic sites of the target proteins. The highest-ranked binding pocket was then selected for docking site for synthetase t-RNA complexes. **Molecular Dynamics Simulation (MDS)** To evaluate the stability of the modeled protein structures, molecular dynamics simulation was performed using the WebGRO server (https://simlab.uams.edu/). The simulation used the GROMOS96 43a1 force field, with the system arranged in a triclinic periodic box and solved using a simple point charge (SPC) water model (Bekker, 1993). To maintain a physiological salt content of 0.15 M, enough amounts of Na^+ and Cl^- ions were supplied. The steepest descent approach was used in 5,000 stages to minimize energy. The simulation was run under constant temperature and pressure (NVT/NPT) conditions of 1.0 bar and 300 K. The data, which spanned 50 nanoseconds (ns) and included 1,000 frames, were examined by measuring the

root mean square deviation (RMSD) with time relative to the initial protein structure. **Results and Discussion** *Z. palmae* has an impressive EtOH production capacity, producing around 2 moles of EtOH per mole of glucose while creating no undesirable byproducts. This efficiency is comparable to that of *Z. mobilis*, a well-known ethanol producer (Aminian & Motamedian, 2023). Notably, while toxic compounds found in lignocellulosic hydrolysates frequently inhibit the growth and enzymatic functions of many bacteria and yeasts involved in saccharification and EtOH production, *Z. mobilis* biofilms have shown increased resistance to these inhibitors (Cao et al., 2023; Shabbir et al., 2023). *Z. palmae*, *Z. mobilis*, and similar species can produce EtOH efficiently under severe environmental conditions. Therefore, investigating the genome of *Z. palmae* and similar bacteria, namely this wild strain of *E. coli* is crucial for modeling and assessing the stability of key enzymes involved in bioethanol production.

Genome sequencing analysis

The CGview program is a popular platform for genome visualization, allowing for the depiction of essential genomic parameters such as GC concentration, GC skew, and gene density. These findings aid in identifying functional and structural sections of the genome, which contributes to our understanding of microbial adaptations and ecological functions in their habitats (Grant & Stothard, 2008; Grin & Linke, 2011). The genome of the investigated organism was found to be around 3 mb in size, with a total ungapped length of 3 Mb. The genetic material was organized across two chromosomes, then assembled into two scaffolds and further divided into two contigs. Notably, both the scaffold and contig N50 values were 3 Mb, implying that at least half of the genome was contained within sequences of this length or greater. The scaffold and contig L50 values were both equal to one, indicating that the genome assembly was complete. The guanine-cytosine (GC) content was determined as 56%, which represents the fraction of these base pairs in the genome. Additionally, genome coverage was recorded at 7.7×, indicating that each base in the genome was sequenced approximately 7.7 times on average. The genome assembly was classified at the "Complete Genome" level, signifying a well-structured and comprehensive representation of the organism's genetic material.

Genome annotation

The genome of *Z. palmae* was annotated using Prokaryotic Genome Annotation Pipeline (PGAP) from the NCBI RefSeq database. PGAP is a powerful genome annotation tool that identifies coding sequences, RNA

genes, and functional elements while maintaining uniform annotations. It also makes it easier to identify microbial genes involved in stress tolerance and biogeochemical cycles (Tatusova et al., 2016). The annotation procedure, which began on February 13, 2024, discovered a total of 2,685 genes, 2,575 of which

encoded proteins. The investigation was carried out with the NCBI PGAP software version 6.6. These computational tools offered useful information on the identified genes and their functional roles within the organism's genomic structure (Figure 1a).
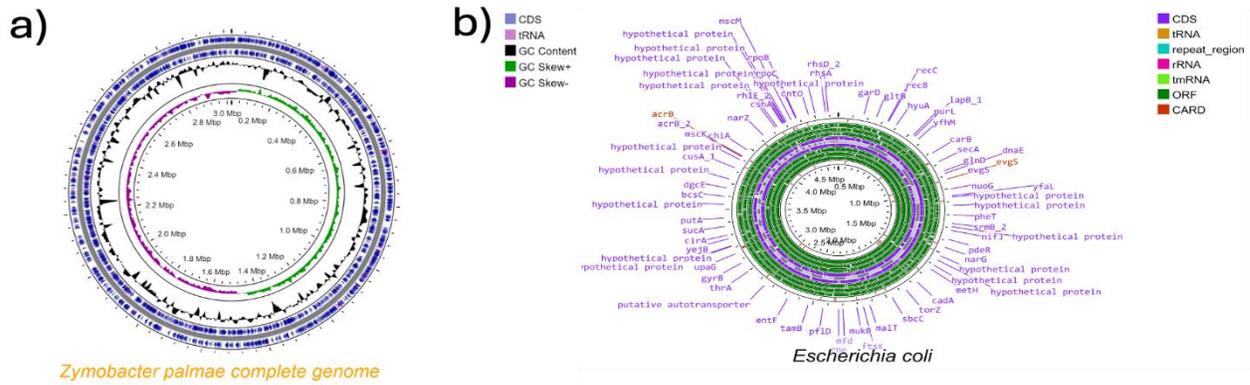

Fig 1. Complete genome structure of *Z. palmae.*

Structure Predictions

The AlphaFold2 tool was used to predict protein structures based on amino acid sequences, with default parameters (Figure 2). AlphaFold2 makes it easier to model protein structures, allowing you to identify variants, active sites, and binding domains. This structural knowledge is critical for understanding the ecological roles and biotechnological possibilities of microbial proteins involved in biosynthetic pathways, biogeochemical cycles, and stress response (Yang et al., 2023; Boland & Ayres, 2024).

Fig 2. Prediction of a protein structure using AlphaFold2 a) cellulase b) lyase and c) protease.

Model confidence was assessed using the pLDDT, which yielded a mean confidence score of 95.2% for the cellulase model, 91.9% for the lyase model, and 93.2% for the protease model. A mean pLDDT score of over 90% suggests a high-confidence model that closely corresponds with empirically confirmed structural data (Jumper et al, 2021). The PROCHECK program was used to examine the correctness and dependability of AlphaFold2-predicted protein structures by evaluating structural attributes such as bond angles, torsion angles, stereochemical accuracy, and Ramachandran plot distribution. This validation phase is critical for ensuring the accuracy of predicted protein structures, especially when researching microbial proteins involved in metabolism, biosynthesis, or stress tolerance. Ensuring structural validity improves the trustworthiness of results in various biological processes (Laskowski et al. 1993; Agnihotry et al. 2022). Figure 3 shows the Ramachandran plot analysis of the predicted protein structure with the PROCHECK program. The Ramachandran plot analysis of the cellulase model revealed that 93.9% of the residues were in the most favorable areas (A, B, and L), with an additional 6.1% in the allowed regions (a, b, l, and p). There were no residues found in the generously authorized (~a, ~b, ~l, and ~p) or banned regions. Similarly, the lyase model showed 87.5% of residues in the most preferred regions, 9.5% in the permissible regions, 2.2% in the generously allowed regions, and 0.7% in the disallowed areas. The protease model has a higher quality structure, with 95.9% of residues in the most preferred areas, 3% in allowed
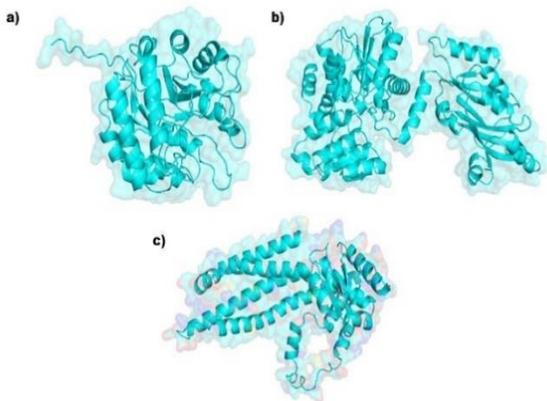
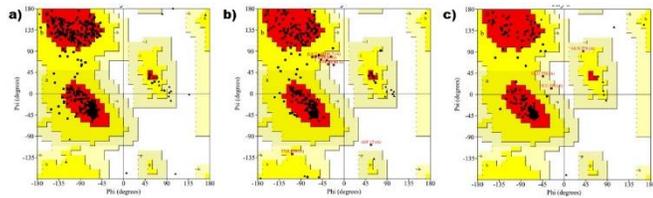regions, 1.1% in generously allowed regions, and none was found in banned regions.

Fig 3. Ramachandran plot in the PROCHECK tool a) cellulase b) lyase and c) protease.

Secondary structure prediction

NetSurfP-2.0 was used to predict protein structural and functional features (surface accessibility, secondary structure, and disordered regions). These predictions are crucial for understanding protein stability, folding, and interaction dynamics (Klausen et al. 2019; Høie et al. 2022). The results revealed that the cellulase protein contains nine helices, 12 strands, and 23 coils. In comparison, the lyase protein has 21 helices, 20 strands, and 39 coils, whereas the protease protein has 12 helices, 4 strands, and 16 coils in its secondary structure (Figure 4).

Fig 4. Prediction of a secondary structure a) cellulase b) lyase and c) protease.

Physicochemical properties of amino acid sequences

The ProtParam tool was used to examine physicochemical properties proteins, such as pI, instability index, aliphatic index, molecular weight, and grand average hydropathicity (GRAVY). These qualities are critical in understanding protein stability, solubility, and functionality. The research revealed that the cellulase structure comprised more negatively charged residues, specifically aspartic acid and glutamic acid, than positively charged residues such as arginine and lysine.

This yielded an isoelectric point of 4.74, indicating an acidic nature. The entire atom count was about 4,751, with 1,535 carbon, 2,348 hydrogen, 402 nitrogen, 459 oxygen, and 7 sulfur atoms.

Lyase protein characteristics

The lyase protein followed a similar pattern to the cellulase protein, with more negatively charged residues—namely aspartic acid and glutamic acid—than positively charged residues such as arginine and lysine. This yielded an isoelectric point of 5.24, indicating a generally acidic nature. The entire atom count was roughly 7,871, with 2,478 carbon, 3,941 hydrogen, 689 nitrogen, 746 oxygen, and 17 sulfur atoms. The computed GRAVY value was -0.094, indicating intrinsic hydrophilicity. While the instability score was 35.21, indicating a tendency toward instability, the protein was classified as stable using standard standards (Mohapatra 2021). Furthermore, measuring the half-life of the protein using its amino acid sequence reveals important information about its stability and prospective functional applications.

In contrast, the protease protein has a unique profile from cellulase and lyase. It contains fewer negatively charged residues (aspartic acid and glutamic acid) and more positively charged residues (arginine and lysine), yielding an isoelectric point of 9.09, indicating a basic character (figure 5).

The entire atom count is roughly 4,656, consisting of 1,473 carbon, 2,345 hydrogen, 407 nitrogen, 411 oxygen, and 20 sulfur atoms. The positive GRAVY value of 0.301 indicates innate hydrophobicity. Despite having an instability index of 24.49, Escuder-Rodríguez et al. (2021) found that the protein is stable in vitro.
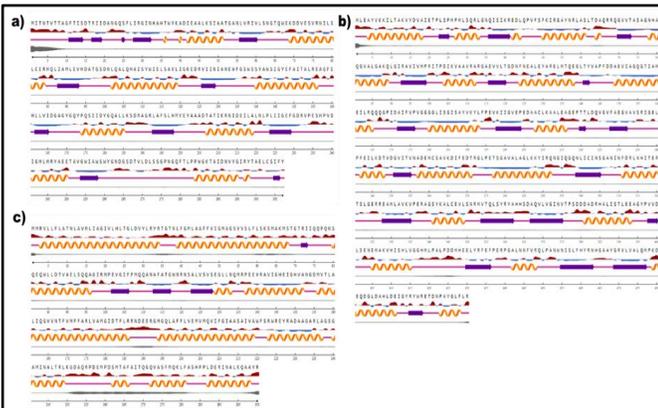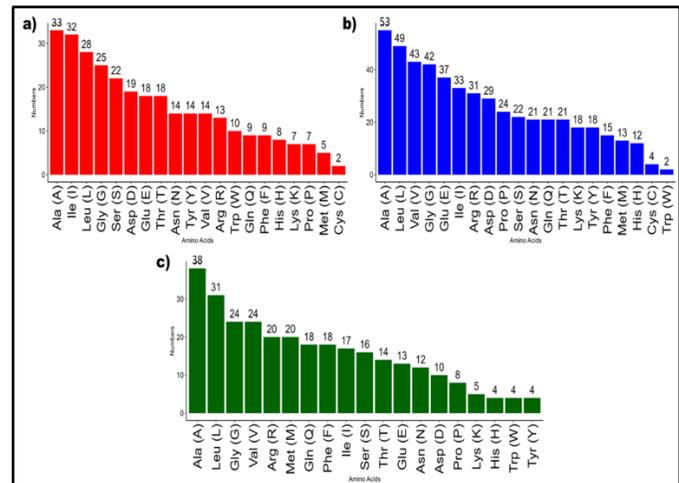

Fig 5. Amino acid composition of the a) cellulase b) lyase and c) protease.

Active site prediction **in** *Z. palmae*

The active-site residues for each protein were identified, providing crucial insights into their functional interactions. For **cellulase** enzyme, the active-site residues include ALA-34, TRP-37, TYR-38, TRP-67, HIS-94, THR-97, ASN-132, GLU-133, TYR-170, GLN-172, GLU-201, GLU-228, ARG-232, TRP-258, GLY-262, ASN-263, ASP-264, and ASP-267. Similarly, the **lyase enzyme** contains active-site residues such as PHE-50, LYS-51, ALA-74, SER-75, ALA-76, GLY-77, ASN-78, HIS-79, GLN-81, PRO-99, PRO-103, LYS-106, PHE-124, LEU-128, TYR-142, PRO-145, PHE-146, ASP-147, VAL-151, GLN-155, PRO-176, GLY-178, GLY-179, GLY-180, GLY-181, LEU-182, GLU-230, GLY-231, VAL-232, ALA-233, VAL-234, SER-235, ARG-236, GLU-276, SER-305, and ASN-308. Additionally, the **protease enzyme** comprises active-site residues such as ALA-111, ASN-112, ALA-113, PHE-114, ALA-115, VAL-143, HIS-146, GLU-147, HIS-150, ASP-155, MET-156, LEU-159, SER-222, ARG-225, GLU-226, MET-242, LEU-246, LEU-249, ALA-253, HIS-284, PRO-285, LEU-287, and ARG-290. These identified active-site residues, visualised in figure 6, highlight the key regions responsible for substrate binding and enzymatic function, essential for understanding their biological roles and potential applications.

Active site prediction **in** *E. coli*

The protease-active- site residues from E. coli are to be THR-184, TYR-208, LYS-209, SER-210, ALA-211, ASP-228, TRP-231, ALA-336, MET-338, PRO-375, GLY-376, GLY- 377, SER-378, VAL-379, MET-406, ALA-408, SER-409, GLY-410, LEU-428, SER-431, GLY-433, ILE-434, PHE-435, PHE-488, and VAL-511. While the the lyase-active- site residues include SER-71, MET-72, ARG-114, ILE-116, LEU-118, LEU-126, GLY-128, THR-130, PRO-151, LEU-152, LEU-191, and GLU-193. These enzymes were also present in *Z. palmae* as documented.

Molecular dynamic simulation

To assess the flexibility and stability of the protein structure predicted by AlphaFold2, a molecular dynamics simulation was run for 50 ns utilising the GROMACS force field and the WebGRO service (Jumper et al. 2021). In protein structural analysis, RMSD is a critical metric for determining molecular stability since it quantifies the average atomic displacement between stacked protein structures. It shows the number of structural changes. The RMSD investigation of the cellulase structure revealed stability at roughly 0.2 nm. The most noticeable variations occurred between 0 and 10 ns, following which
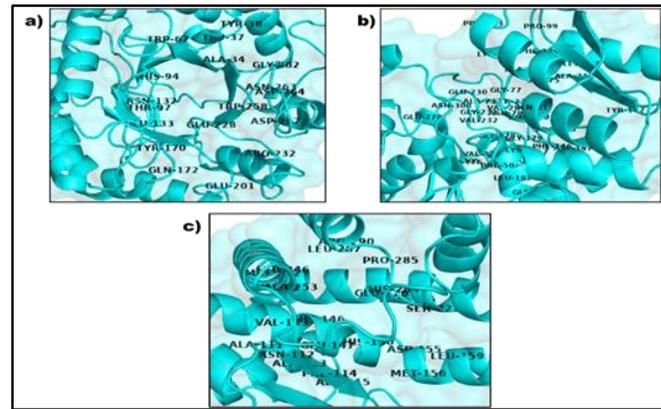

Fig 6. Active site for proteins. The bind site representing the cavity enlarged to unveil the amino acid residues predicted by web server a) cellulase b) lyase and c) protease.
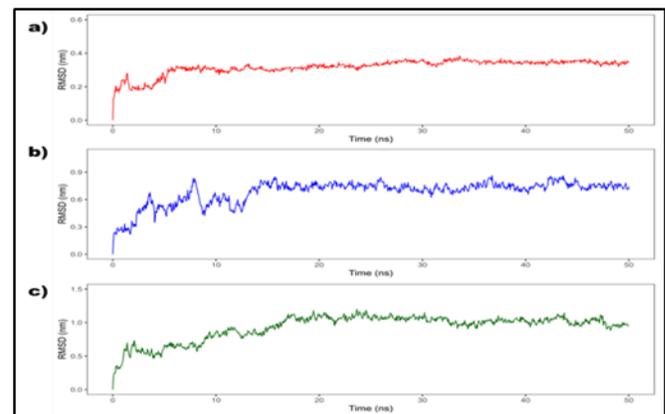

Fig 7. Molecular dynamic simulation RMSD results in a) cellulase b) lyase and c) protease.

the readings steadied at 10 ns, retaining an average RMSD of 0.35 nm (figure 7a). Similarly, the RMSD study of the lyase structure revealed stability at around 0.8 nm. The most notable variations occurred between 0 and 15 ns, following which the structure stabilized with an average RMSD of 0.8 nm from 15 to 50 ns (Figure 7b). Similarly, the protease structure achieved equilibrium at 0.5 nm, with the most significant oscillations occurring between 0 and 17 ns. Beyond this time, the readings remained stable, with an average RMSD of 1 nm spanning 17 ns to 50 ns (Figure 7c). A low RMSD value indicates minimal structural variation, implying a well-defined and stable protein structure. This stability indicates a compact and energetically advantageous arrangement of amino acids, which increases the protein's resistance to environmental disturbances (Babayan-Mashhadi et al. 2024).

Implementation and limitation of the study

The computational frameworks used in this study provide precise insights and can be used to optimize a variety of biotechnological industrial-scale processes, including bioethanol production (Raajaraam & Raman 2022; Ranganathan et al. 2022).

This study provides critical data by examining the structural features of major ethanol-producing enzymes, which can be used to provide the groundwork for future experimental studies targeted at confirming enzyme functions, improving reaction conditions, and increasing bioethanol yield. The data indicate that *Z. palmae* has tremendous promise as a long-term bioethanol-producing bacterium. Despite the promising results, the predicted enzyme structures have not yet been experimentally validated. To establish enzyme activity and functional functions in ethanol synthesis, computational predictions must be supported by laboratory tests (Wang et al. 2020). Furthermore, structural comparisons were limited due to a lack of previously detailed structural data. The study did not look at enzyme-substrate interactions in real-world fermentation circumstances, such as inhibitor stability, temperature and pH changes, and cofactor requirements. Although molecular dynamics simulations showed structural stability, extended simulation times and more situations could provide a more thorough review. Furthermore, reliance on a single organism for ethanol production may provide scalability issues, as industrial fermentation processes sometimes include competition with different bacteria. Addressing these challenges will require extensive pilot studies and comparisons with established fermentation systems (Tse et al. 2021). Despite the promising results, the predicted enzyme structures have not yet been experimentally validated. To establish enzyme activity and functional functions in ethanol synthesis, computational predictions must be supported by laboratory tests (Wang et al. 2020). Furthermore, structural comparisons were limited due to a lack of previously detailed structural data. The study did not look at enzyme-substrate interactions in real-world fermentation circumstances, such as inhibitor stability, temperature and pH changes, and cofactor requirements. Although molecular dynamics simulations showed structural stability, extended simulation times and more situations could provide a more thorough review. Furthermore, reliance on a single organism for ethanol production may provide scalability issues, as industrial fermentation processes sometimes include competition with different bacteria. The synthesizing protein and translation mechanism is wide-ranging and captivating. The ribosomal RNA (rRNA) and associated proteins are of course gene products. The RNA polymerase and transfer RNA (tRNA) of *Escherichia coli* are therefore capable of serving the key adapter role to the mechanism of translation (Watson, J.D., F.H.C. Crick. 1953). This also brings to notice that ethanologenic wild strain like *Escherichia coli* can produce almost the theoretical yield of ethanol as like *Z. palmae*.

Declarations
Conflict of interest
The authors declare that they have no conflict of interest.

References

Abatángelo V, Peressutti Bacci N, Boncompain CA, Amadio AA, Carrasco S, Suárez CA, Morbidoni HR. (2017). Broad-range lytic bacteriophages that kill Staphylococcus aureus local field strains. Plos One 12.

Abdelhadi IM.A, Sofy A.R, Hmed AA, Refaey EE, Soweha HE, Abbas MA. (2021). Discovery of Polyvalent Myovirus (vB_STM-2) Phage as a Natural Antimicrobial System to Lysis and Biofilm Removal of Salmonella Typhimurium Isolates from Various Food Sources. Sustainability 13.

Accolas JP, Spillmann H. (1979). The Morphology of Six Bacteriophages of Streptococcus thermophilus. Journal of Applied Bacteriology 47:135-144.

Ackermann HW. (2012). Bacteriophage Electron Microscopy. Pages 1-32 Bacteriophages, Part A.

Ahmadi H.D, Radford A, KropinskiM, Lim LT, Balamurugan S. (2017). Thermal-Stability and Reconstitution Ability of Listeria Phages P100 and A511. Frontiers in Microbiology 8.

Ahn J, Kim S, Jung LS, Biswas D. (2013). In Vitro Assessment of the Susceptibility of Planktonic and Attached Cells of Foodborne Pathogens to Bacteriophage P22-Mediated Salmonella Lysates. Journal of Food Protection 76:2057-2062.

Akya A, Chegene Lorestani R, Shahveisi-zadeh J and, Bozorgomid A. (2020). <p>Antimicrobial Resistance ofStaphylococcus aureus Isolated from Hospital Wastewater in Kermanshah,

Iran</p>. Risk Management and Healthcare Policy Volume 13:1035-1042.

Alonzo F, Torres VJ. (2014). The Bicomponent Pore-Forming Leucocidins of Staphylococcus aureus. Microbiology and Molecular Biology Reviews 78:199-230.

Anany HEJ, Lingohr A, Villegas HW, AckermannY M. She Griffiths.MW, Kropinski AM.(2011). A Shigella boydii bacteriophage which resembles Salmonella phage ViI. Virology Journal 8.

Ansari SHP, Nepal R, Gauta N. Rayamajhi S, Shrestha, G, Upadhya A, Acharya H, Chapagain ML (2014). Threat of drug resistant Staphylococcus aureus to health in Nepal. BMC Infectious Diseases 14.

Bannerman TLK, Kleeman T, Kloos WE. (1993). Evaluation of the Vitek Systems Gram-Positive Identification card for species identification of coagulase-negative staphylococci. Journal of Clinical Microbiology 31:1322-1325.

Barylski JF, Enault BE, DutilhMB. P, Schuller RA, Edwards A, Gillis J, Klumpp P, Knezevic M, Krupovic JH, Kuhn R, Lavigne HM, Oksanen, MB, Sullivan HB, Jang P, Simmonds P, Aiewsakun J, WittmannITolstoy J, RBrister A, Kropinski M, Adriaenssens EM, Jarmiin L. (2020). Analysis of Spounaviruses as a Case Study for the Overdue Reclassification of Tailed Phages. Systematic Biology 69:110-123.

Bauer AW, Kirby WM, Sherris JC, Turck M (1966). Antibiotic susceptibility testing by a standardized single disk method. Am J Clin Pathol 45:493-496.

BekirK FB, Abdallah A, Ellafi A, Bakhrouf A. (2011). Adherence assays and slime production of Staphylococcus aureus strains after their incubation in seawater microcosms. Annals of Microbiology 61:819-823.

Bibi Z, Abbas Z, Rehman Su. (2016). The phage P.E1isolated from hospital sewage reduces the growth ofEscherichia coli. Biocontrol Science and Technology 26:181-188.

Boswihi SS, Udo EE. (2018). Methicillin-resistant Staphylococcus aureus : An update on the epidemiology, treatment options and infection control. Current Medicine Research and Practice 8:18-24.

Brown S, Santa Maria JP, Walker S. (2013). Wall Teichoic Acids of Gram-Positive Bacteria. Annual Review of Microbiology 67:313-336.

Chambers HF, DeLeo FR. (2009). Waves of resistance: Staphylococcus aureus in the antibiotic era. Nature Reviews Microbiology 7:629-641.

Chang, Shin YH, Lee JH, Park C, Paik SY, Ryu S. (2015). Isolation and Genome Characterization of the Virulent Staphylococcus aureus Bacteriophage SA97. Viruses 7:5225-5242.

Cheesbrough M. (2006). District laboratory practice in tropical countries. Cambridge University Press (CUP): Cambridge, UK.

Chessa M, Ganau DG, Mazzarello V. (2015). An overview of Staphylococcus epidermidis and Staphylococcus aureus with a focus on developing countries. The Journal of Infection in Developing Countries 9:547-550.

Cornelissen APJ, Ceyssens J, T'Syen H, Van Praet, JP, Noben O, Shaburova V, Krylov VN,Volckaert, G, Lavigne R. (2011). The T7-Related Pseudomonas putida Phage φ15 Displays Virion-Associated Biofilm Degradation Properties. Plos One 6.

Darch SEKN, Kragh EA, Abbott T, Bjarnsholt JJ, Bull M, Whiteley, Sperandio V. (2017). Phage Inhibit Pathogen Dissemination by Targeting Bacterial Migrants in a Chronic Infection Model. mBio 8.

Domingo-Calap P, Delgado-Martínez J. (2018). Bacteriophages: Protagonists of a Post-Antibiotic Era. Antibiotics 7.

Echeverría-Vega AP, Morales-Vicencio C, Saez-Saavedra, Gordillo-Fuenzalida F, Araya R. (2019). A rapid and simple protocol for the isolation of bacteriophages from coastal organisms. MethodsX 6:2614-2619.

Else TA, Pantle CR, Amy PS. (2003). Boundaries for Biofilm Formation: Humidity and Temperature. Applied and Environmental Microbiology 69:5006-5010.

FDA. (2002). Bacteriological Analytical Manual. Food and Drug Administration: Arlington, VA, USA.

Funke G, Funke-Kissling P. (2005). Performance of the New VITEK 2 GP Card for Identification of Medically Relevant Gram-Positive Cocci in a Routine Clinical Laboratory. Journal of Clinical Microbiology 43:84-88.

Ganaie MYS, Qureshi Z, Kashoo SA, Wani MI, Hussain R, Kumar M, Maqbool R, Sikander P, Banday MS,. Malla WA,. Mondal P, Khan RIN. (2018). Isolation and characterization of two lytic bacteriophages against Staphylococcus aureus from India: newer therapeutic agents against Bovine mastitis. Veterinary Research Communications 42:289-295.

García PC, Madera B, Martínez A, Rodrígue z, Evaristo J, Suárez M. (2009). Prevalence of bacteriophages infecting Staphylococcus aureus in dairy samples and their potential as biocontrol agents. Journal of Dairy Science 92:3019-3026.

Golkar ZO, Bagasra, Pace DG. (2014). Bacteriophage therapy: a potential solution for the antibiotic

resistance crisis. The Journal of Infection in Developing Countries 8:129-136.

Gorski A, Miedzybrodzki R, Borysowski J, Weber B -Dabrowska M, Lobocka, W Fortuna, Letkiewicz S, Zimecki M, Filby G. (2009). Bacteriophage therapy for the treatment of infections. Curr Opin Investig Drugs 10:766-774.

Gudin IG, Zeleke D, Woyessa, Kassa T. (2018). Isolation of Bacteriophage and Assessment of its Activity against Biofilms of Uropathogenic *Escherichia coli* in Jimma Town, South Western Ethiopia. American Journal of Current Microbiology 6:52-66.

Guo ZJ, Huang G, Yan L, Lei S, Wang L, Zhou YuL, Gao A, Feng X,. Han W,. Gu J, Yang J. (2017). Identification and Characterization of Dpo42, a Novel Depolymerase Derived from the *Escherichia coli* Phage vB_EcoM_ECOO78. Frontiers in Microbiology 8.

Gupta PP, Gupta G, Mittal RK, Agarwal M, Goyal R, (2015). Detection of biofilm production in blood culture isolates ofStaphylococci. International Journal of Medical Research & Health Sciences 4.

Gutiérrez DL, Rodríguez-Rubio B, Martínez A. Rodríguez A, García P. (2016). Bacteriophages as Weapons Against Bacterial Biofilms in the Food Industry. Frontiers in Microbiology 7.

Holt JN, Krieg P, SneathJ Staley, Williams S, (2000). Bergey's Manuel of Determinative Bacteriology. Lippincott Williams & Wilkins: Philadelphia, PA, USA.

Ingmer HD, Gerlach C, Wolz VA, Fischetti RP, Novick, Ferretti J, Portnoy DA, Braunstein M, Rood JI. (2019). Temperate Phages of Staphylococcus aureus. Microbiology Spectrum 7.

Islam MA, Uddin MS, Islam MJ., Ahmed MU, Alam MM. (2021). Investigation of antibiotic resistance pattern of Staphylococcus aureus in clinical samples of animals and humans from selective areas of Bangladesh. Bangladesh Journal of Veterinary Medicine 19.

Jamalludeen NR,. Johnson P, Friendship RAM. Kropinski EJ, Lingohr, Gyles CL, (2007). Isolation and characterization of nine bacteriophages that lyse O149 enterotoxigenic *Escherichia coli*. Veterinary Microbiology 124:47-57.

Jepson CD, March JB. (2004). Bacteriophage lambda is a highly stable DNA vaccine delivery vehicle. Vaccine 22:2413-2419.

Jończyk EM, Kłak R, Międzybrodzki M and, Górski A (2011). The influence of external factors on bacteriophages—review. Folia Microbiologica 56:191-200.

Kaur SK, Harjaiand S, Chhibber M. (2012). Methicillin-Resistant Staphylococcus aureus Phage Plaque Size Enhancement Using Sublethal Concentrations of Antibiotics. Applied and Environmental Microbiology 78:8227-8233.

Kaźmierczak Z, Górski A, Dąbrowska K. (2014). Facing Antibiotic Resistance: Staphylococcus aureus Phages as a Medical Tool. Viruses 6:2551-2570.

Khawaja KA, Rauf M, Abbas Z, Rehman Su. (2016). A virulent phage JHP against Pseudomonas aeruginosa showed infectivity against multiple genera. Journal of Basic Microbiology 56:1090-1097.

Knezevic P, Petrovic O. (2008). A colorimetric microtiter plate method for assessment of phage effect on Pseudomonas aeruginosa biofilm. Journal of Microbiological Methods 74:114-118.

Kostaki MN, Chorianopoulos,. Braxou E,. Nychas GJ, Giaouris E. (2012). Differential Biofilm Formation and Chemical Disinfection Resistance of Sessile Cells of Listeria monocytogenes Strains under Monospecies and Dual-Species (with Salmonella enterica) Conditions. Applied and Environmental Microbiology 78:2586-2595.

Kraushaar BM,. Thanh D,. Hammerl JA,. Reetz J, Fetsch A, Hertwig S. (2013). Isolation and characterization of phages with lytic activity against methicillin-resistant Staphylococcus aureus strains belonging to clonal complex 398. Archives of Virology 158:2341-2350.

Krömker V. (2006). Kurzes Lehrbuch Milchkunde und Milchhygiene, 1st ed.; Stuttgart: Parey, Germany.

Kwiatek M, Parasion S, Mizak L, Gryko R, Bartoszcze V and, Kocik J. (2012). Characterization of a bacteriophage, isolated from a cow with mastitis, that is lytic against Staphylococcus aureus strains. Archives of Virology 157:225-234.

Latka A, Drulis-Kawa A. (2020). Advantages and limitations of microtiter biofilm assays in the model of antibiofilm activity of Klebsiella phage KP34 and its depolymerase. Scientific Reports 10.

Lau, MW, Gunawan C, Balan V. et al. (2010). Comparing the fermentation performance of *Escherichia coli* KO11, Saccharomyces cerevisiae 424A(LNH-ST) and Zymomonas mobilis AX101 for cellulosic ethanol production. Biotechnol Biofuels **3**, 11.

Laverty GS, Gorman P, Gilmore BF. (2013). Biomolecular Mechanisms of Staphylococcal Biofilm Formation. Future Microbiology 8:509-524.

Lavigne R, Darius P, Summer EJ, Seto D, Mahadevan P, Nilsson AS, Ackermann HW, Kropinski AM. (2009). Classification of Myoviridae bacteriophages

using protein sequence similarity. BMC Microbiology 9.

Leid, JG. (2009). Bacterial Biofilms Resist Key Host Defenses. Microbe 4:66-70.

Li X, Gerlach D, Du X, Larsen J, M. Stegger MP, Kühner P, Peschel A, Xia G, Winstel V. (2015). An accessory wall teichoic acid glycosyltransferase protects Staphylococcus aureus from the lytic activity of Podoviridae. Scientific Reports 5.

LuT K, and, Koeris MS. (2011). The next generation of bacteriophage therapy. Current Opinion in Microbiology 14:524-531.

Lungren MP, Christensen D, Kankotia R, Falk I, Paxton BE, Kim CY. (2013). Bacteriophage K for reduction of Staphylococcus aureusbiofilm on central venous catheter material. Bacteriophage 3.

Mattila S, Ruotsalainen P, Jalasvuori M. (2015). On-Demand Isolation of Bacteriophages Against Drug-Resistant Bacteria for Personalized Phage Therapy. Frontiers in Microbiology 6.

Melo L, Brandão A, Akturk E, Santos S, Azeredo J. (2018). Characterization of a New Staphylococcus aureus Kayvirus Harboring a Lysin Active against Biofilms. Viruses 10.

Mlynarczyk -Bonikowska B, Kowalewski C, Krolak -Ulinska A, Marusza W. (2022). Molecular Mechanisms of Drug Resistance in Staphylococcus aureus. International Journal of Molecular Sciences 23.

NCCLS/CLSI. (2007). Performance Standards for Antimicrobial Susceptibility Testing. National Committee for Clinical Laboratory Standards/Clinical and Laboratory Standards Institute: Wayne, MI, USA.

Neopane P, Nepal HP, Shrestha R, Uehara O, Abiko Y. (2018). In vitro biofilm formation by Staphylococcus aureus isolated from wounds of hospital-admitted patients and their association with antimicrobial resistance. International Journal of General Medicine Volume 11:25-32.

O'Flaherty S, Ross RP, Flynn J, Meaney WJ, Fitzgerald GF, Coffey A. (2005). Isolation and characterization of two anti-staphylococcal bacteriophages specific for pathogenic Staphylococcus aureus associated with bovine infections. Letters in Applied Microbiology 41:482-486.

O'Flynn G, Coffey A, Fitzgerald GF, Ross RP. (2006). The newly isolated lytic bacteriophages st104a and st104b are highly virulent against Salmonella enterica. Journal of Applied Microbiology 101:251-259.

O'Neill J. (2014). Antimicrobial Resistance: Tackling a Crisis for the Health and Wealth of Nations. Review on Antimicrobial Resistance.

Oliveira H, Melo LD. R,. Santos SB NóbregaFL, Ferreira EC, Cerca N, Azeredo J, LD. Kluskens LD. (2013). Molecular Aspects and Comparative Genomics of Bacteriophage Endolysins. Journal of Virology 87:4558-4570.

Olsen MC, Thiran E, Hasler T, Vanzieleghem T, Belibasakis GN, Mahillon J, Loessner MJ, Schmelcher M. (2018). Synergistic Removal of Static and Dynamic Staphylococcus aureus Biofilms by Combined Treatment with a Bacteriophage Endolysin and a Polysaccharide Depolymerase. Viruses 10.

Olszak T, Shneider MM, Latka A, Maciejewska B, Browning C, Sycheva LV, Cornelissen A, Danis K, Wlodarczyk S, Senchenkova N, Shashkov AS, Gula G, Arabski M, Wasik, S, Miroshnikov KA, Lavigne R, Leiman PG, YA, Knirel YA, Drulis-Kawa Z. (2017). The O-specific polysaccharide lyase from the phage LKA1 tailspike reduces Pseudomonas virulence. Scientific Reports 7.

Pires D, Oliveira PH, Melo LD. R,. Sillankorva S, J. Azeredo. (2016). Bacteriophage-encoded depolymerases: their diversity and biotechnological applications. Applied Microbiology and Biotechnology 100:2141-2151.

Pujato S, Guglielmotti ADM, Martínez -García MA, Quiberoni M, Mojica FJ. (2017). Leuconostoc mesenteroides and Leuconostoc pseudomesenteroides bacteriophages: Genomics and cross-species host ranges. International Journal of Food Microbiology 257:128-137.

Quinn P, Markey BK, Carter M, Donnelly W, Leonard F, Maguire D. (2002). Veterinary microbiology and microbial disease. Iowa State Univ. Press, Blackwell Science Ltd.

Rodríguez-Rubio L, Martínez B, Donovan DM, Rodríguez A, García P. (2012). Bacteriophage virion-associated peptidoglycan hydrolases: potential new enzybiotics. Critical Reviews in Microbiology 39:427-434.

Sangha KK, Kumar BVS, Agrawal RK, Deka D, Verma R. (2014). Proteomic Characterization of Lytic Bacteriophages of Staphylococcus aureus Isolated from Sewage Affluent of India. International Scholarly Research Notices 2014:1-6.

Sharma D, Misba L, Khan AU. (2019). Antibiotics versus biofilm: an emerging battleground in microbial communities. Antimicrobial Resistance & Infection Control 8.

Sharma S, Chatterjee S, Datta S, Prasad R, Dubey D, Prasad RK, Vairale MG. (2017). Bacteriophages and its applications: an overview. Folia Microbiologica 62:17-55.

Shi Y, Yan Y, Ji W, Du B, Meng X,. Wang H, Sun J. (2012). Characterization and determination of holin protein of Streptococcus suis bacteriophage SMP in heterologous host. Virology Journal 9.

Sofy AR, Abd El Haliem NF, Refaey EE, Hmed AA. (2020). Polyvalent Phage CoNShP-3 as a Natural Antimicrobial Agent Showing Lytic and Antibiofilm Activities against Antibiotic-Resistant Coagulase-Negative Staphylococci Strains. Foods 9.

Sofy AR, El-Dougdoug NK, Refaey EE, Dawoud RA, Hmed AA. (2021). Characterization and Full Genome Sequence of Novel KPP-5 Lytic Phage against Klebsiella pneumoniae Responsible for Recalcitrant Infection. Biomedicines 9.

Sommer J, Trautner C, Witte AK, Fister S, Schoder D, Rossmanith P, Mester PJ. (2019). Don't Shut the Stable Door after the Phage Has Bolted—The Importance of Bacteriophage Inactivation in Food Environments. Viruses 11.

Spricigo D, Bardina AC, Cortés P, Llagostera M. (2013). Use of a bacteriophage cocktail to control Salmonella in food and the food industry. International Journal of Food Microbiology 165:169-174.

Standardization GI. (1995). Microbiological Milk Testing Determination of the Bacterial Count–Part 5: Spatula Method; DIN 10192-5:1995-05. German Institute for Standardization: Berlin, Germany.

Stepanović .S, Vuković D, Hola V, Bonaventura GD,. Djuki Ć S, Ćirković I, Ruzicka F. (2007). Quantification of biofilm in microtiter plates: overview of testing conditions and practical recommendations for assessment of biofilm production by staphylococci. Apmis 115:891-899.

Stewart PS, Costerton WJ. (2001). Antibiotic resistance of bacteria in biofilms. The Lancet 358:135-138.

Szafrański SP, Winkel A, Stiesch M. (2017). The use of bacteriophages to biocontrol oral biofilms. Journal of Biotechnology 250:29-44.

Tadesse BT, Ashley EA, Ongarello S, Havumaki J, WijegoonewardenaI M, González J, Dittrich S. (2017). Antimicrobial resistance in Africa: a systematic review. BMC Infectious Diseases 17.

Tait K, Skillman LC, Sutherland IW. (2002). The efficacy of bacteriophage as a method of biofilm eradication. Biofouling 18:305-311.

Takeuchi IK, Osada A, Azam H, Asakawa H, Miyanaga K, Tanji Y, Pettinari MJ. (2016). The Presence of Two Receptor-Binding Proteins Contributes to the Wide Host Range of Staphylococcal Twort-Like Phages. Applied and Environmental Microbiology 82:5763-5774.

Tan CS, Aqiludeen NA, Tan R, Gowbei A, Mijen AB,. Santhana Raj L, Ibrahim SF. (2020). Could bacteriophages isolated from the sewage be the solution to methicillin-resistant Staphylococcus aureus? Med J Malaysia 75:110-116.

Tomat D, Casabonne C, Aquili V, Balagué C, Quiberoni A. (2018). Evaluation of a novel cocktail of six lytic bacteriophages against Shiga toxin-producing *Escherichia coli* in broth, milk and meat. Food Microbiology 76:434-442.

Tond D. (2021). Novel Targets and Mechanisms in Antimicrobial Drug Discovery. Antibiotics 10.

Uchiyama JI, Takemura-Uchiyama Si, Kato M, Sato T, Ujihara H, Matsui M, Hanaki H, Daibata M, Matsuzaki S. (2014). In silico analysis of AHJD-like viruses, Staphylococcus aureus phages S24-1 and S13′, and study of phage S24-1 adsorption. MicrobiologyOpen 3:257-270.

Wang Z, Zheng P, Ji W, Fu Q, Wang H,. Yan Y, Sun J. (2016). SLPW: A Virulent Bacteriophage Targeting Methicillin-Resistant Staphylococcus aureus In vitro and In vivo. Frontiers in Microbiology 7.

Waters EM, Neill DR, Kaman B, Sahota JS, Clokie MR.J, Winstanley C, Kadioglu A. (2017). Phage therapy is highly effective against chronic lung infections withPseudomonas aeruginosa. Thorax 72:666-667.

Watson, J.D., F.H.C. Crick. 1953. Genetical implications of the structure of deoxyribonucleic acid. Nature 171:964 –67.

White R, Chiba S, Pang T, Dewey JS, Savva CG, Holzenburg A, Pogliano K, Young R. (2011). Holin triggering in real time. Proceedings of the National Academy of Sciences 108:798-803.

Willis JA, Cheburkanov V, Chen S, Soares JM,. Kassab G, Blanco KC, Bagnato VS, Figueiredo P, Yakovlev VV. (2022). Breaking down antibiotic resistance in methicillin-resistant Staphylococcus aureus: Combining antimicrobial photodynamic and antibiotic treatments. Proceedings of the National Academy of Sciences 119.

Xia G, Corrigan RM, Winstel V, Goerke CC, Gründling A, Peschel A. (2011). Wall Teichoic Acid-Dependent Adsorption of Staphylococcal Siphovirus and Myovirus. Journal of Bacteriology 193:4006-4009.

Yau JW, Thor SM, Tsai D, Speare T, Rissel C. (2021). Antimicrobial stewardship in rural and remote primary health care: a narrative review. Antimicrobial Resistance & Infection Control 10.

Young D, Hussell T, Dougan G. (2002). Chronic bacterial infections: living with unwanted guests. Nature Immunology 3:1026-1032.

Zeng D, Debabov D, Hartsell TL, Cano RJ, Adams S, Schuyler JA, McMillan R, Pace JL. (2016). Approved Glycopeptide Antibacterial Drugs: Mechanism of Action and Resistance. Cold Spring Harbor Perspectives in Medicine 6.

Zhang Q, Xing S, Sun Q, Pei G, Cheng S, Liu Y, An X,. Zhang X, Qu Y, Tong Y. (2017). Characterization and complete genome sequence analysis of a novel virulent Siphoviridae phage against Staphylococcus aureus isolated from bovine mastitis in Xinjiang, China. Virus Genes 53:464-476.